IJEMME

INTERNATIONAL JOURNAL of ELECTRONICS, MECHANICAL and MECHATRONICS ENGINEERING

Year: **2020** Volume **10** Number **2**

VISUAL DESIGN & ACADEMIC STUDIES COORDINATION OFFICE

Nabi SARIBAŞ - Selin YILMAZ - Elif ERMAN

PRINTED BY

Renk Matbaası Basım ve Ambalaj San. Tic. A.Ş.
Ziya Gökalp Mah. Süleyman Demirel Bulvarı İş Modern D Blok No:27D D:D8 34104 Başakşehir / İstanbul

ISSN: 2146-0604

International Journal of Electronics, Mechanical and Mechatronics Engineering (IJEMME) is peer-reviewed journal which provides a platform for publication of original scientific research and applied practice studies. Positioned as a vehicle for academics and practitioners to share field research, the journal aims to appeal to both researchers and academicians.

Internationally indexed by EBSCO and DOAJ

CONTENTS

From the Editor

International Journal of Electronics, Mechanical and Mechatronics Engineering (IJEMME), is an international multi-disciplinary journal dedicated to disseminate original, high-quality analytical and experimental research articles on Robotics, Mechanics, Electronics, Telecommunications, Control Systems, System Engineering, Biomedical and Renewable Energy Technologies. Contributions are expected to have relevance to an industry, an industrial process, or a device. Subject areas could be as narrow as a specific phenomenon or a device or as broad as a system.

The manuscripts to be published are selected after a peer review process carried out by our board of experts and scientists. Our aim is to establish a publication which will be abstracted and indexed in the Engineering Index (EI) and Science Citation Index (SCI) in the near future. The journal has a short processing period to encourage young scientists.

Prof. Dr. Hasan HEPERKAN
Editor

INTERNATIONAL JOURNAL OF ELECTRONICS, MECHANICAL AND MECHATRONICS ENGINEERING
Vol.10Num.2-2020 (1763-1771)

Control For a DC Micro grid Feeding Uncertain Loads in More Electric Aircraft

Abdel Rahman El Samarji[1], Murtaza FARSADI[2]

1.Abstract

This project proposes an improved hybrid solar and wind with battery management system with specialized and accurate controllers developed using PID controller, the main concern of the project is developing an intelligent system which will work in synchronization with all other components of microgrid. The algorithm is developed in such a way that all sources should operate according to the variable load conditions. [1]We have proposed algorithm which is efficient in terms of making system reliable and stable, we have involved renewable resources as solar and wind energy for generation thus saving fuel consumption ultimately it affects economy of country. Simulation has been done which demonstrate the whole scenario of operation of all components of microgrid. Simulation model consists of model of renewable sources and battery with its controller grid and Load. To test the effectiveness of the system it is simulated on MATLAB. We can analyze the system effectiveness at different conditions namely as step changes in irradiance and several load condition.

2.Introduction

A microgrid is basically designed to overcome some challenges in distribution networks such as fuel consumption, reliability of system equipment, increment in emissions. A microgrid consists of renewable sources, battery, grid, load and control system for synchronization. Energy management system controller is developed using PID for better performance. We are using renewable resources

[1] *Electrical Electronics Engineering, Engineering Faculty, Istanbul Aydin University, Istanbul, Turkey, raiomar@stu.aydin.edu.tr*

[2] *Application and Research Centre for Advanced Studies, Istanbul Aydin University, Istanbul, Turkey, murtazafarsadi@aydin.edu.tr*

DOI: 10.17932/IAU.IJEMME.2010.001/ijemme_v10i2001

as solar which are available in abundance. We have developed modules of both the resources to check their effectiveness in the proposed system. It is very important to design efficient energy management system because it provides stable power to electrical vehicle and other portable devices. [2] A battery management basically consists of charging and discharging strategies, SoC performance of the battery at different scenario, voltage balancing. The algorithm developed for energy management system is based on simple architecture that battery should be in charging mode when there is availability of solar power, battery comes in discharging mode when there is less availability of Pv power to compensate load.

[3]SOC estimations play very important role in whole energy management system, Soc estimation decides when battery should attain charging mode and discharging mode. It also ensures battery performance at different conditions. Advanced algorithm is implemented in the control system for a microgrid that can optimize the energy absorptions, save energy, as well as reduce costs ultimately energy management system. The main objective of the proposed system is to check the effectiveness of control strategies developed using PID controller in Microgrid for the purpose of energy management system. We have developed algorithm for the improvisation of energy management system in a Microgrid.

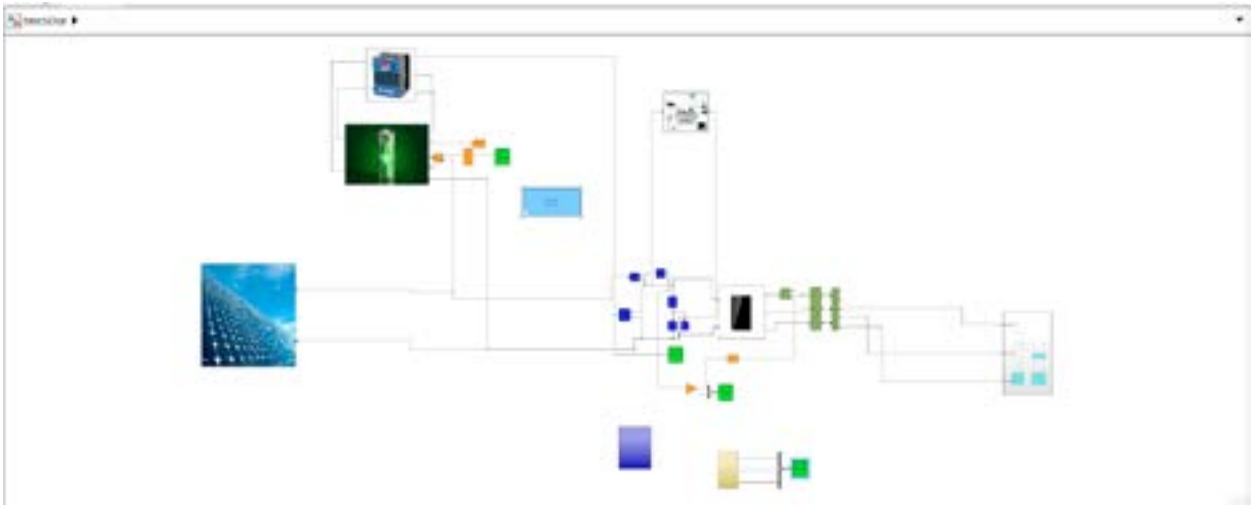

Figure 1: Proposed Simulink Model of the system

Renewable Resources of Energy

Solar energy is used as renewable source of energy for the system.

Solar Source-The solar source is used to generate power from the sun rays. A photovoltaic system makes use of some or more solar panels to convert the solar energy into electricity. It consists of various components which include the photovoltaic modules, mechanical and electrical connections and mountings and means of regulating and/or modifying the electrical output.

MATHEMATICAL MODELLING

1. PV Farm -

The equivalent circuit of a PV cell is shown in Fig. 1. The current source Iph represents the cell photocurrent. Rsh and Rs are the intrinsic shunt and series resistances of the cell, respectively. Usually, the value of Rsh is very large and that of Rs is very small, hence they may be neglected to simplify the analysis. Practically, PV cells are grouped in larger units called PV modules and these modules are connected in series or parallel to create PV arrays which are used to generate electricity in PV generation systems. The equivalent circuit for PV array is shown in Fig. 2.

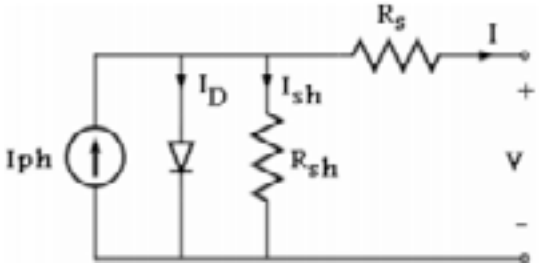

Fig. 1

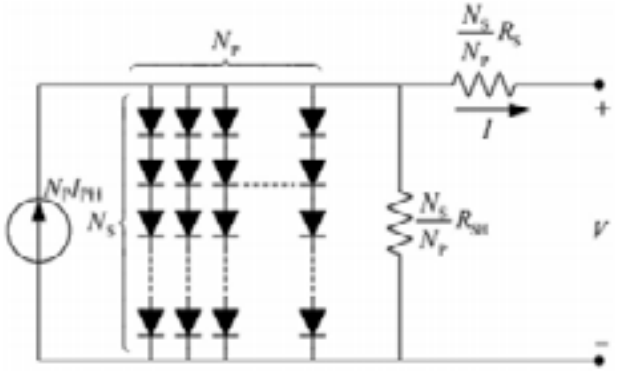

Fig.2

The voltage–current characteristic equation of a solar cell is provided: Module photo-current Iph:

$$I_{ph} = [I_{sc} + K_i(T - 298)] \times Ir/1000 \qquad (1)$$

Here, Iph: photo-current (A); Isc: short circuit current (A) ;Ki: short-circuit current of cell at 25 °C and 1000 W/m2

T: operating temperature (K); Ir: solar irradiation (W/m2)

Module reverse saturation current Irs:

$$I_{rs} = I_{sc}/[\exp(qV_{OC}/NskmT) - 1] \qquad (2)$$

Here, q: electron charge, = 1.6 × 10−19C; Voc: open circuit voltage (V); Ns: number of cells connected in series; n: the ideality factor of the diode; k: Boltzmann's constant, = 1.3805 × 10−23 J/K.

The module saturation current I0 varies with the cell temperature, which is given by:

$$I_0 = I_{rs}\left[\frac{T}{T_r}\right]^3 \exp\left[\frac{q \times E_{g0}}{nk}\left(\frac{1}{T} - \frac{1}{T_r}\right)\right] \quad (3)$$

Here, Tr: nominal temperature = 298.15 K; Eg0: band gap energy of the semiconductor, = 1.1 eV; The current output of PV module is:

$$I = N_P \times I_{ph} - N_P \times I_0 \times \left[\exp\left(\frac{V/N_S + I \times R_s/N_P}{n \times V_t}\right) - 1\right] - I_{sh} \quad (4)$$

With

$$V_t = \frac{k \times T}{q} \quad (5)$$

and

$$I_{sh} = \frac{V \times N_P/N_S + I \times R_S}{R_{sh}} \quad (6)$$

Here: Np: number of PV modules connected in parall; R s: series resistance (Ω); Rsh: shunt resistance (Ω);Vt: diode thermal voltage (V).

3. RESEARCH METHOD

An improvised control system is developed to improve microgrid stability and to increase performance efficiency at different scenarios. Proposed system consists of solar panels, grid, load and Nickel cadmium battery with its controller (initial soc of battery is set as 95%).

Overview of the algorithm is shown below which consists of two different cases-

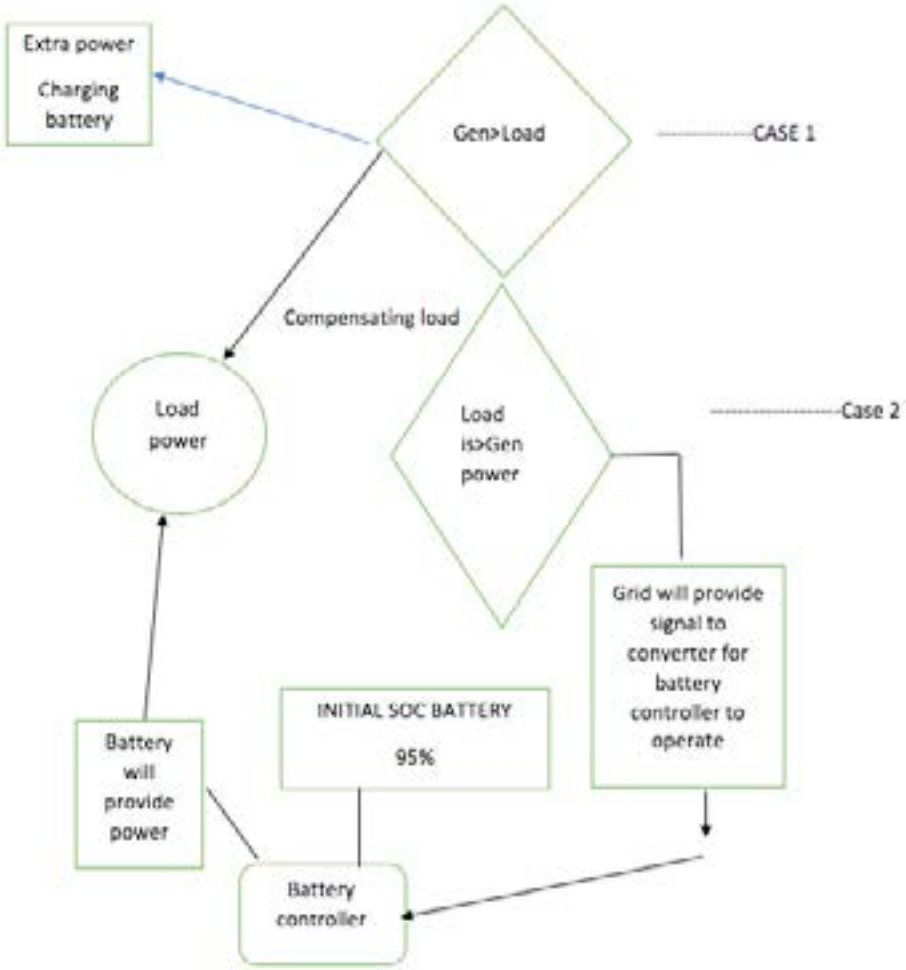

CASE 1-

- If Generating power is more than the Load then extra power will be used in charging batteries and remaining will compensate load.

CASE 2-

- If load is greater than generating power grid will provide signal to the converter for battery controller to operate, converter is designed with fuzzy logic control
- Charged battery will provide power to the load.

Control system

This is basic control system for switching process of battery to operate at different time according to the load and other resources.

Here, two parameters of battery are taken into consideration that are voltage and battery Soc,

- Initial Soc of battery 95% and response time 30 second that means whenever soc reach to 90%, it indicates that battery is fully charged.

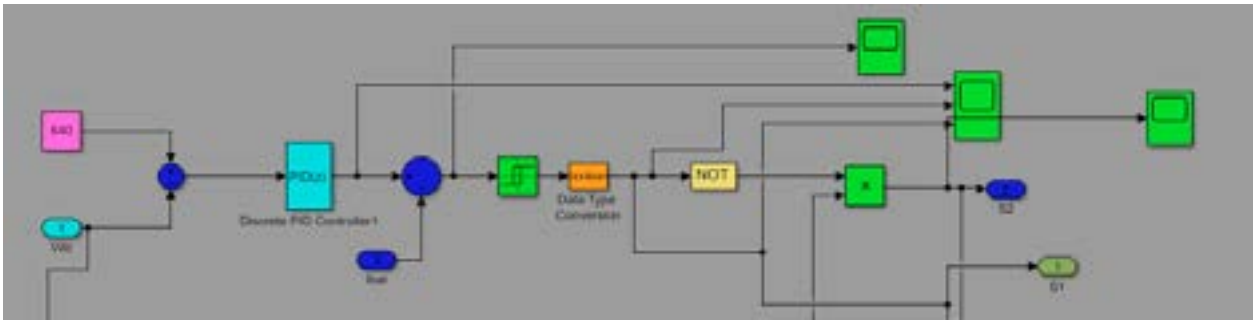

This part is for voltage regulation of the battery this part will decide when voltage to increase and when to drop, whenever it senses load power is not compensated by other resources then it provides pulse to the switches s1 and s2. In this input to the PID is the comparison value of vdc and reference value.

PID works to achieve desired value. It provides switching pulses through s1 and s2 which in input to the mosfe

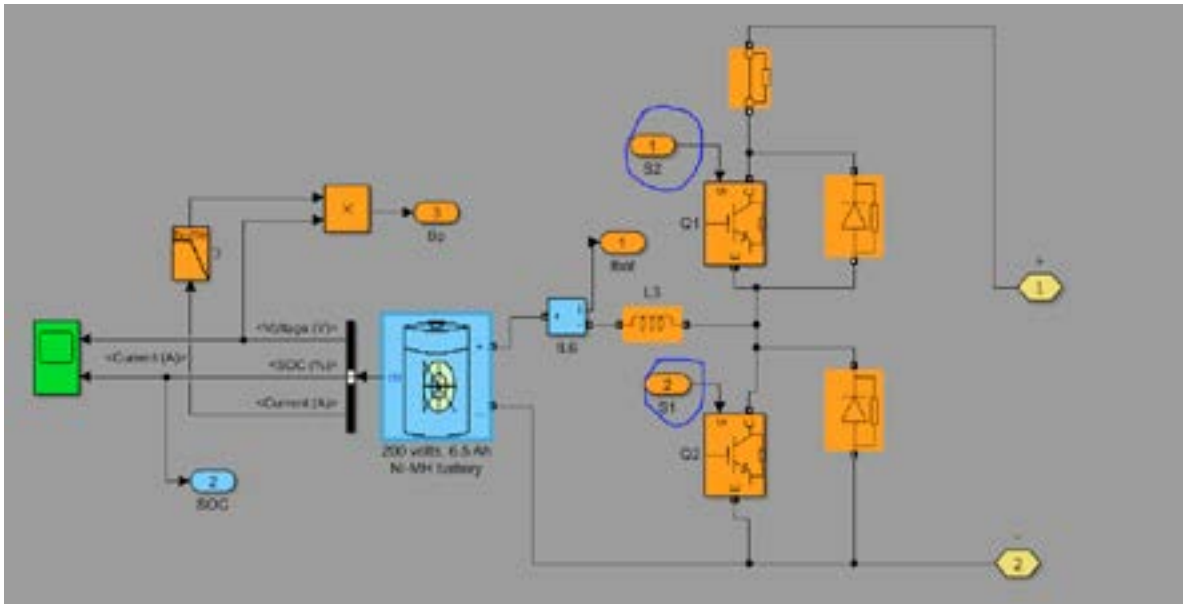

Battery management using soc control system here input is soc of the current situation. In next step, it is compared with some value of Soc, that whenever the soc reached its minimum it provides pulses to s1 and s2 for recharging of battery.

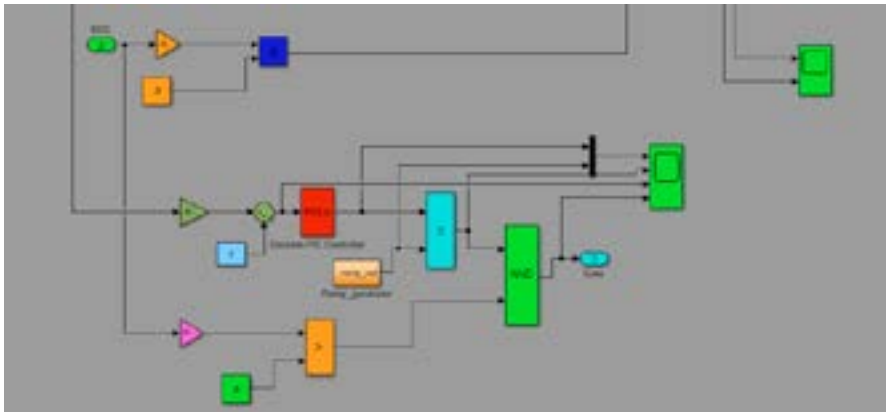

With the hybrid voltage and current mode control, the inverter is controlled as a current source to generate the reference power in the grid-tied mode. And its output power should be the sum of the power injected to the grid and the load demand P load + jQ load, which can be expressed as follows by assuming that the load is represented as a parallel RLC circuit:

$$P_{\text{load}} = \frac{3}{2} \cdot \frac{V_m^2}{R} \tag{1}$$

$$Q_{\text{load}} = \frac{3}{2} \cdot V_m^2 \cdot \left(\frac{1}{\omega L} - \omega C \right) \tag{2}$$

In the overall block diagram for the proposed unified control strategy, where the inductor current iLabc, the utility voltage vg abc, the load voltage cvarci, and the load current iLLabc are sensed. And the three phase inverter is controlled in the SRF, in which, three phase variable will be represented by dc quantity. The control diagram is mainly composed by the inductor current loop, the PLL, and the current reference generation module. In the inductor current loop, the PI compensator is employed in both D- and Q-axes, and a decoupling of the cross coupling denoted byω0Lf/k PWM is implemented in order to mitigate the couplings due to the inductor. The output of the inner current loop dd q, together with the decoupling of the capacitor voltage denoted by 1/k PWM, sets the reference for the standard space vector modulation that controls the switches of the three-phase inverter. It should be noted that k PWM denotes the voltage gain of the inverter, which equals to half of the dc voltage in this paper.

The PLL in the proposed control strategy is based on the SRF PLL, which is widely used in the three-phase power converter to estimate the utility frequency and phase. Furthermore, a limiter is inserted between the PI compensator GPL Land the integrator, in order to hold the frequency of the load voltage within the normal range in the islanded operation. In Fig., it can be found that the inductor current is regulated to follow the current reference iLrefdq, and the phase of the current is synchronized to the grid voltage vgabc. If the current reference is constant, the inverter is just controlled to be a current source, which is the same with the traditional grid-tied inverter. The new part in this paper is the current reference generation module shown in Fig, which regulates the current reference to guarantee the power match between the DG and the local load and enables

the DG to operate in the islanded mode. Moreover, the unified load current feed forward, to deal with the nonlinear local load, is also implemented in this module.

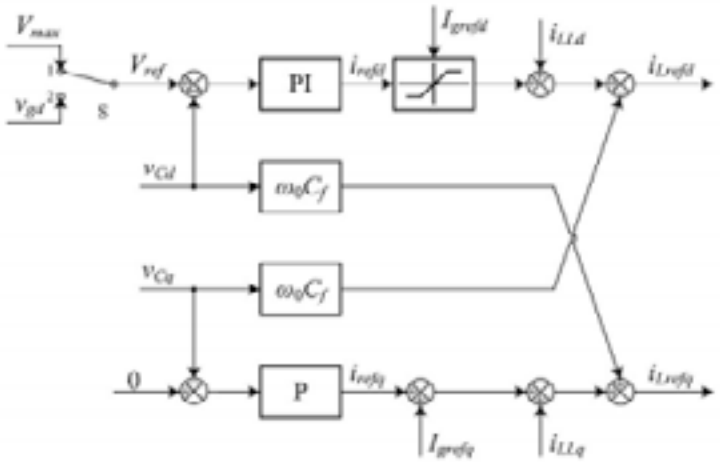

Fig. Black diagram of the current generation module

Results

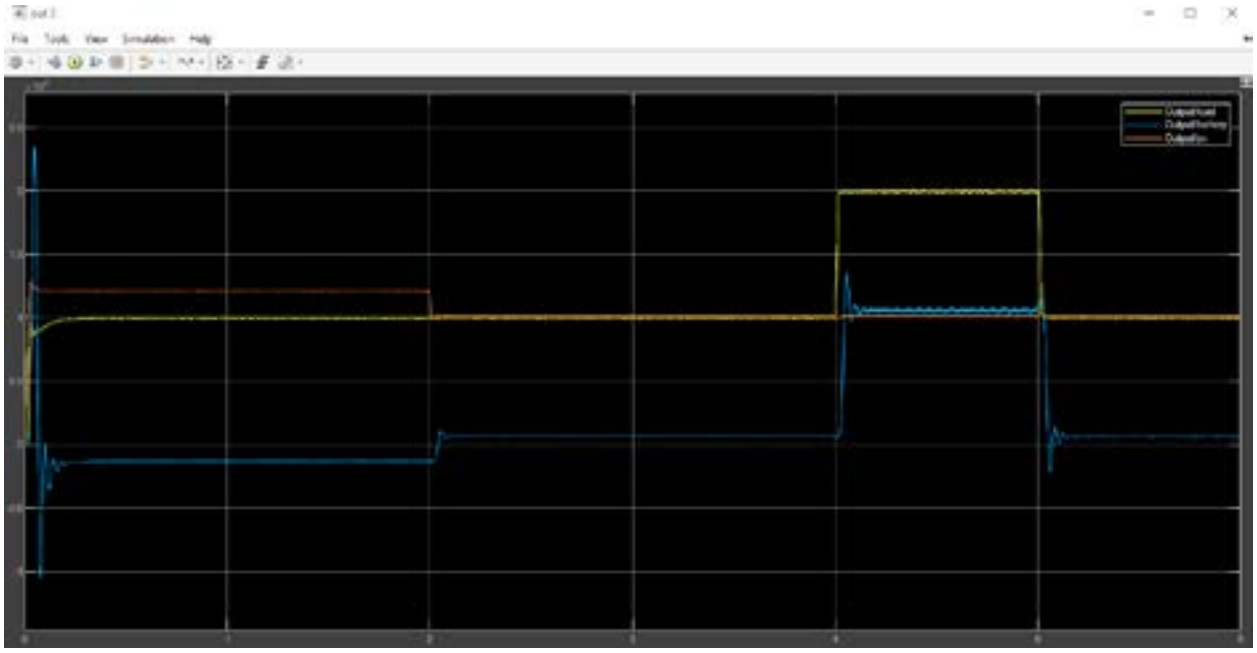

Above From the graph we can see charged battery is providing power to load and battery is charged by the renewable resources that is solar. Extra power is transferred to the grid sometimes it takes power from other sources. At starting the solar power is very less this is because of solar data i.e. irradiance data has small values at starting time.

Here is the output of all pV, load and battery. Here, controller performed battery management, we can observe at starting battery is charging mode since load is compensated by PV power, but after sometime when we load increases the battery comes in discharging mode at time 4 sec to 5 sec after that again it gets stable.

Initially, battery is charged so it is providing enough power to compensate the load, whenever others resources provide enough power to load, battery comes into charging mode.

Conclusion

Modeling of each components of Microgrid is presented and focused on EMS with pid controller. We have used Nickel-Metal hydride type battery because of its high-power capability. Performance of the proposed system has been evaluated at different electrical conditions.

Control structure is designed in such a way that it can perform good at any sudden changes in load and disturbance. Simulation results show effectiveness and the credibility of control system designed using PID controller.

References

[1] A. M. S. A. Alias Khamis, "Modeling and Simulation of Small Scale Microgrid System," Australian Journal of Basic and Applied Sciences, pp. 412-421, 2012.

[2] S. M. R. G.-M. I. ,. E. F. Robert Salas-Puente * ID, "Practical Analysis and Design of a Battery Management System for a Grid-Connected DC Microgrid for the Reduction of the Tariff Cost and Battery Life Maximization," 19 July 2018.

[3] 1. J. A. P.-M. S. C.-A. A. S. J. P. a. A. I. B. Juan José Martínez, "Development and Application of a Fuzzy Control System for a Lead-Acid Battery Bank Connected to a DC Microgrid," International Journal of Photoenergy, vol. 2018, p. 14.

INTERNATIONAL JOURNAL OF ELECTRONICS, MECHANICAL AND MECHATRONICS ENGINEERING
Vol.10 Num.2 - 2020 (1773-1783)

Mechanical Examination of Fly Ash and Zeolite-Based Geopolymer Mortars

Mehmet Fatih ALTAN[1], Gökan AKYOL[2]

Abstract

This study intends to study compressive and flexural strength properties, Ultrasonic Pulse Velocity (UPV), weight changes, and splitting tensile of geopolymer mortar made with fly-ash and zeolite as binder materials, silica sand and basalt stone powder as filler materials with different ratios (25%, 50%, and 75%). The prepared geopolymer mortar was activated by sodium silicate and sodium hydroxide solutions (12mol) and the Ground granulated blast-furnace slag was added with 13% of the completely prepared mix. The suggested specimens were exposed to compressive and flexural strength test at 7, 28, 56 days, weight changes were investigated after the 28th day, the splitting tensile test was tested at 28 and 56 days while the Ultrasonic Pulse Velocity tests was examined during 3, 7, 28, and 56 days.

The acquired experimentally results reveal that all the manufactured geopolymer mix's compressive and flexural strength properties increase with time and the highest value was attended on the 56th day. Moreover, the weight changes value were between 7.70% and 9.19%, splitting tensile test increase at the 56th day and were between 3.94 and 5.13 same as ultrasonic Pulse Velocity through time and the highest value was obtained on the 56th day for B2 mix with 4134 m/s.

Keywords: *Geopolymer, binder, fly-ash, zeolite, strength properties, UPV.*

1. Introduction

In general, an alkali-activated cement is mainly composed of an alkaline liquid solution (for example soda or sodium silicate) and a chemically reactive pulverulent solid, made for example of blast furnace slag or clays calcined, which are sources of reactive aluminum and/or calcium silicates (Fu et al., 2012). As for Portland cement, additives (plasticizers, etc.) can be added to them, in particular, to implement them (Dupuy et al., 2019). Geopolymers are special cases of alkali-activated cement. Although the term geopolymer was proposed by (Davidovits et al., 1991).

[1] *Department of Civil Engineering, Istanbul Aydin University, Turkey, e-mail: mehmetaltan@aydin.edu.tr*
[2] *Department of Civil Engineering, Istanbul Aydin University, Istanbul, Turkey.*
DOI: 10.17932/IAU.IJEMME.2010.001/ijemme_v10i2002

This term defines a group of predominantly amorphous inorganic materials, having an aluminum-silicate skeleton, based on SiO2 and Al2O3. An alternative term is "inorganic polymer cement" or inorganic polymer cement (IPC) (Kamseu et al., 2012). Geopolymers are among the alkali-activated materials poor in calcium Ca (Gharzouni et al., 2018). They are often qualified as "green cement", on the one hand, due to the low emission of CO2 into the atmosphere, linked to their manufacture (Kenne Diffo et al., 2015), and on the other hand, their compressive strength, which may be similar or superior to that of certain Portland cement mortars or concretes (Cyr & Pouhet, 2015). Geopolymers are the product of a reaction between an alumino-silicate source and an alkaline or acidic activator solution. The materials used as the alumino-silicate source can be activated clays (by calcination at more than 500 ° C) (Kenne Diffo et al., 2015), such as metakaolin, obtained from kaolinite), fly ash (Criado et al., 2010), silica fume or a mixture of these different sources (Krivenko et al., 2007). The alumino-silicate source is usually in the form of a solid powder, and it is the only component that provides aluminates to the geopolymer (Duxson et al., 2007). The alumino-silicate source also provides silicates, but the reaction between aluminates and silicates, giving the geopolymer, must be activated chemically.

The activation solutions are:

- Acids, such as phosphoric acid (H3PO4) (Célerier et al., 2018) or mixtures of acids.
- Alkaline solutions such as sodium hydroxide (NaOH), potassium hydroxide (KOH), or an alkaline silicate of the type (n SiO2 -m M2O) where M is an alkaline cation (generally Na, K, or even Cs or Li).

In what follows, the alkali-activated binders with alkali silicates (Hajjaji et al., 2013), for which the literature is abundant and which have the best performance. Their behavior and performance are the best known and could be applied industrially for the design of grouts for the treatment of solids entering reservoir rocks.

In general, the chemical composition of a geopolymer can be written as:

$$aAl_2O_3 - bSiO_2 - cM_2O - nH_2O$$

with a, b, c, and n being the mole amounts of aluminates, silicates, alkaline activator, and water, respectively, and M the type of alkaline activator (usually Na, K, Li, or Cs). Sodium and potassium are the most commonly used activators. In the literature, the different formulations are expressed using molar ratios, which are either (1) those of the oxides, for example, SiO2/ Al2O3 (Chen et al., 2005), or (2) the chemical elements, for example, Si / Al. In the case of aluminum and silicon, there is a factor of two between the molar ratios of the element and those of the oxide. For example, a molar Si / Al equal to 1.8 corresponds to a molar $SiO_2 / Al_2O_3 = 3.6$.

In (Zhang et al., 2014) notably, the molar ratio (SiO2 / M2O) of an alkali silicate, where M is an alkali metal, is expressed as an oxide ratio and called the modulus of the silicate.

To evaluate the properties of geopolymers concerning the stresses of oil wells, for which Portland cements are usually used, (Elder et al., 2013) proposed composition limits for geopolymers based on metakaolin and solution. sodium-based activator (M = Na).

The fly ash from the incineration of household waste is made up of a large number of chemical compounds, some of which - based on heavy metals: lead, cadmium, etc. - are a threat to the

environment. The properties of fly ash differ depending on the characteristics of the coal and the method of burning. It is generally useful as an additive in cement and concrete by showing pozzolanic properties due to its siliceous and aluminous composition. It increases the workability of fresh concrete due to its fine and spherical grains; it also reduces the heat of hydration. By reacting with the lime formed as a result of cement hydration, it forms an additional binder gel, fills the gaps in the cement paste, and adds strength to the concrete. Lime rate in fly ash obtained by burning lignite coal is generally high and such ashes also show hydraulic, ie binding properties. The deliberate use of fly ash in various fields provides an economic advantage for both the user and the ash producer, and the environment is protected as waste material is removed.

In addition, the user gains various technical advantages in new products or applications they produce. Despite all these positive aspects, the amount of fly ash evaluated using it cannot exceed a small percentage of the amounts obtained in the power plants, and the world average is around 15%. Zeolite is an aqueous alumina silicate crystal of porous, alkali (Na and K) and alkaline earth (Ca) elements with a three-structure network. The smallest structural unit of any zeolite crystal is SiO_4 or AlO_4 tetrahedra (He et al., 2012). Single and double ring secondary structure units and high symmetry parameters are formed by the combination of primary structure units formed by Si and Al tetrahedra. By arranging these polieder and secondary structure units in different shapes in three dimensions(Kong et al., 2007), a zeolite skeleton with micropores emerges.

Main physical and chemical properties of zeolites (Ranjbar et al., 2015); There is an ion change, adsorption and related molecular sieve structure, silica content, and also light color and lightness in sedimentary zeolites.

The structures of zeolites contain voids and have a honeycomb or lattice appearance. Cations and water, which are generally alkali and alkaline earth metals, can be found in cavities (Oh et al., 2010). The honeycomb or lattice structure of zeolites has a channel or gap size between 2-12 Ao. Since cations are weakly bound to the zeolite, they can easily exchange ions, so zeolites are used as ion exchangers (He et al., 2013). The water molecules in the pores can also be easily heated, leaving the zeolitic structure, or can be re-adsorbed.

Natural zeolites are a group name consisting of more than 40 minerals. The most known of these are; It is analcime, chabasite, clinoptilolite, erionite, ferrierite, heulandite, mordenite, stilbite, and phylipsite, laumonite, natrolite, faujasite, synthetic zeolite, synthetic zeolite X.

There are also synthetic zeolites. Pure and properly structured synthetic zeolites were first synthesized in 1938, and their production was carried out in 1948. These are not equivalent to natural zeolites and there are 200 types. These zeolites, especially detergent and consumed in the chemical industry in Turkey are not output at this time.

This work presents a geopolymer mortar manufactured by fly-ash and zeolite as binder materials activated with chemical solutions sodium silicate and sodium hydroxide, while as filler materials basalt stone powder were used replaced silica sand with different ratio (25%, 50%, and 75%). The mechanical performance of the manufactured geopolymer specimens was conducted at 7, 28, and 56 days. Visual appearance, the strength properties, UPV, weight changes, and splitting tensile of the manufactured samples were obtained experimentally.

2. Materials and Methods

In this work, fly ash and zeolite were used as binder materials silica sand and basalt stone powder was used as filler materials. Liquid sodium silicate (SiO_2/(Na)_2O = 3.29 M) ratio and sodium hydroxide (12mol) was once used for alkaline activation taken from AS Kimya (Istanbul/Turkey). The sodium hydroxide was prepared by adding 1liter of distilled water to 480g of sodium hydroxide pellets to obtain 12mol. The obtained sodium hydroxide was stored at room temperature for 24 hours before being used with sodium silicate/sodium hydroxide in a 2:1 ratio. To enhance the tenacity of the mix blast furnace slag was used. Basalt samples were homogenized and dried at 105°C for 24 hours. From INCI Group Company (Sakarya/Turkey) the basalt powder stone was extracted. In this work as aggregate, the silica sand with less than 0,25 mm particle diameter was used correspondent to TS 706 EN 12620. The mixing procedure has been finished, the mortar was used to the molds 50x50x50 mm, 40x40x160 prisms, and 300*150 mm cylinders and vibrated, and then the geopolymer samples were kept for 24h in the ambient temperature. All the specimens were held for 24 hours in the drying oven at 100°C. After the curing, the samples were preserved in room temperature conditions. Moreover, the mechanical tests, compressive strength test according to ASTM C 109 was executed after 7, 28, and 56 days utilizing the 50x50x50 mm cubes, and the Flexural strength test quoted by ASTM C 348 utilizing the 40x40x160 prisms samples was carried also after 7, 28 and 56 days (Nikolić et al., 2015).

Table 1: The Fly ash, zeolit, and slag chemical properties.

Chemical Analysis(%)	SiO_2	Al_2O_3	Fe_2O_3–	TiO_2	CaO	MgO	K_2O	Na_2O	SO_3
Fly-Ash	59,94	22,87	4,64	0,94	3,08	1,55	2,19	0,62	0,35
Zeolite	71	-	1,70	-	3,40	1,42	2.70	-	-
Slag	40,55	12,83	1,1	-	32,58	5,87	-	0,79	0,18

Table 2. Sodium silicate chemical properties.

Chemical Analysis (%)	NaOH	Na_2CO_3	CL	SO_4	Al	Fe
SH	99,1	0,3	≤0,01	≤0,01	≤0,002	≤0,002

Table 3. Sodium hydroxide chemical propertimes

Chemical Analysis (%)	SiO_2	Na_2O	Fe (%)	Density (g/ml)	Heavy metals (%)
SS	27,0	8,2	≤0,005	1360	≤0,005

Table 4. Silica sand and basalt stone powder chemical properties

ChemicalAnalysis (%)	SiO_2	Al_2O_3	Fe_2O_3	TiO_2	CaO	CaO_2	K_2O	Na_2O	SO_3
Silica sand	99,70	0,17	0,016	-	0,01	92,9	-	-	-
Basalt stone powder	56,9	17,6	8,1	0,9	7	-	1,9	3,8	-

Table 5. Mix of control sample geopolymer composites (g)

Fly ash	zeolite	Slag	SS (Si)	SH (NaOH (12 mol))	Silica Sand
700	300	133	667	333	2000

Table 6. The mix of basalt stone powder replacing silica sand with different ratios (g).

Fly ash	Zeolit	Slag	Si	NaOH (12mol)	Silica sand	Basalt powder
700	300	133	667	333	1500	500
					1000	1000
					500	1500

3. Results and Discussion

The mixes were named as following control (100% silica sand), B1 (75% silica sand and 25% basalt powder), B2 (50% silica sand and 50% basalt powder) and B3 (25% silica sand and 75% basalt powder).

Fig. 1. The manufactured geopolymer samples

3.1. Strength properties

Table 7. Compressive strength results (Mpa) at 7, 28 and 56 days.

Mix ID	7 days	28 days	56 days
Control	60,21	65,34	66,11
B1	62,84	67,27	68,08
B2	65,33	69,77	72,15
B3	63,12	65,44	66,79

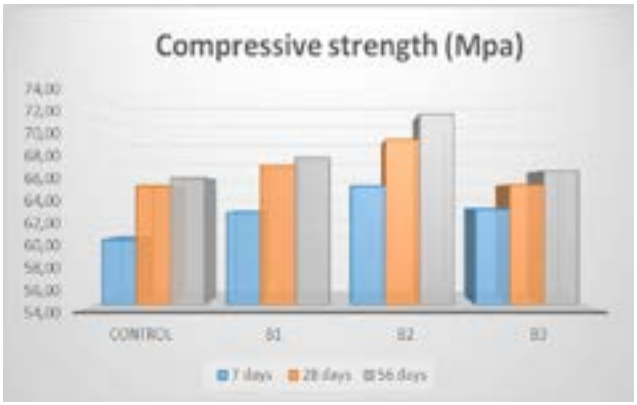

Fig. 2. The diagram of compressive strength for the manufactured samples

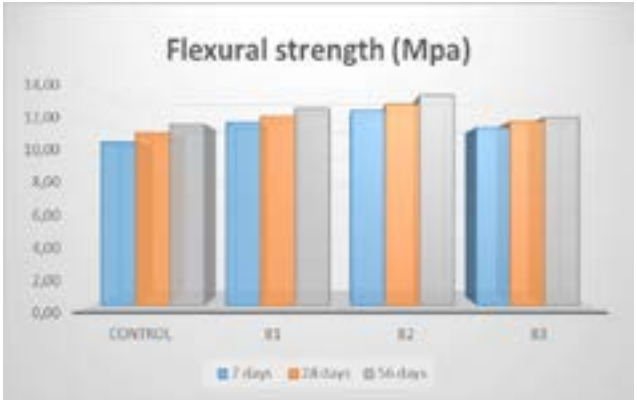

Fig. 3. The diagram of Flexural strength for the manufactured samples

Table 8. Flexural strength results (Mpa) at 7, 28 and 56 days.

Mix ID	7 days	28 days	56 days
Control	10,66	11,23	11,81
B1	11,94	12,34	12,87
B2	12,72	13,13	13,72
B3	11,59	11,98	12,25

The different combinations used in this work affect the results of compressive and flexural strength, Four samples were mixed with basalt powder and partial replacement of silica sand was observed as a new class in sequence to consider the acquired results. Tables 7 and 8 show the results below. According to compressive strength, the mixes with partial replacement of basalt powder with a ratio of 50% (B2) confirmed higher consequences when in contrast to 100% silica sand as a control mix. The combination of 25% basalt powder (B1) satisfied demonstrated a changeable achievement from 7 to 56 days, the same as 75% basalt (B3). Also, the results obtained for the mixe of 50% basalt powder (B2) 7 to 56 days the performance increased with time and the final result was 72.15 Mpa. Furthermore, the samples show an increase in flexural strength and the best results obtained was 50% basalt powder (B2) with a value of 13.72 Mpa at 56 days. The whole results are showin in Fig.2, Fig.3, Table 7, and Table 8.

3.2.Water absorption and porosity

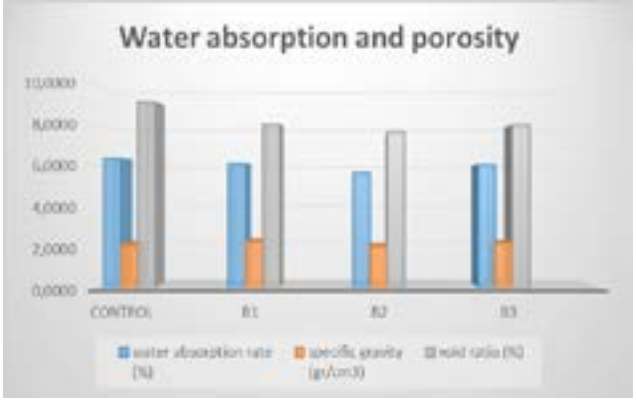

Fig. 3. The diagram of Flexural strength for the manufactured samples

Observing the physical properties of manufactured geopolymer sample about the water absorption and porosity of control sample 6.93% in terms of porosity 9.19% of water absorption. The basalt stone powder samples (B1, B2, B3) confirmed good overall performance in contrast with the control samples, the values were 6.11%, 5.67%, and 6.06% respectively for porosity and 8.08%, 7.70%, and 8.03% of water absorption respectively, The fine particles of basalt stone powder could explain the behavior bellow and provide a good transportation property of the matrix.

3.3 Ultrasonic pulse velocity

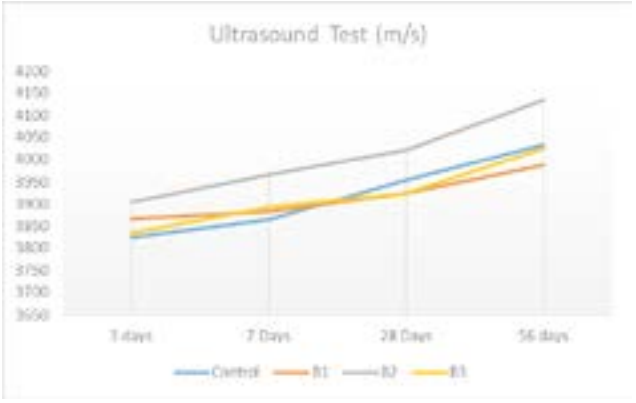

Fig.4. Ultrasonic pulse velocity values (m/s).

To investigate the homogeneity of the matrix, the ultrasonic pulse velocity test was investigated. Fig 4 shows the result obtained (Chakkor & Altan), as can be remarked B2 (50% basalt stone powder + 50% silica sand) sample confirmed a certain boom in velocity and, besides they exceedingly yielded higher effects in contrast with the other mixes the value yielded were 3905 m/s, 3965 m/s, 4022 m/s, and 4134 m/s respectively for 3, 7, 28 and 56 days. B1 and B3 mixes showed an increase from 3 to 56 days and the final value was 3988 m/s and 4025 m/s respectively. Furthermore, the control sample yielded 3825 m/s, 3864 m/s, 3955 m/s and 4034m/s respectively for 3, 7, 28 and 56 days.

3.4. Split tensile strength

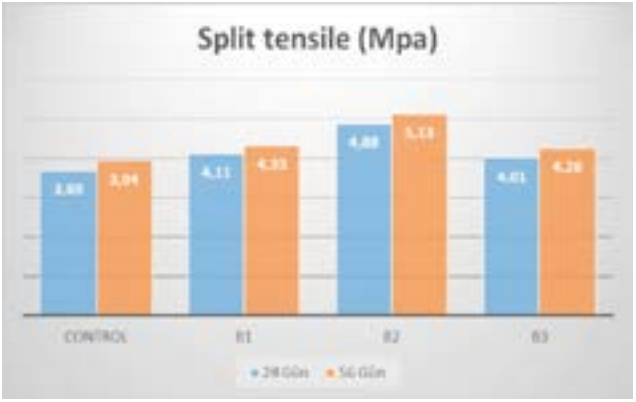

Fig.5. Ultrasonic pulse velocity values (m/s).

The split tensile strength of the manufactured geopolymer mortar samples with different filler ratios of silica sand and basalt stone powder related to 28 and 56 days is shown in the bar diagram in Fig.5. From the bar diagram the geopolymer mortar sample B2 blended with 50% basalt powder and 50% silica sand shown maximum split tensile strength values from the other mixes with 4.88 Mpa and 5.13 Mpa. Moreover, it was observed that the split tensile strength for the other mixes B1 and B3 increases gradually with age from 28 to 56 days.

4. Conclusion

The current work propose was to study the mechanical composition impact of adding basalt stone powder as a filler material with silica sand with different ratios (25%, 50%, and 75%), and the main binder materials of this study, fly ash and zeolite based on geopolymer composites.

Moreover, the experimental study approved that by observing compressive and flexural strength a significant increase estimate was obtained in terms of time 7, 28, and 56 days for all the manufactured samples. Furthermore, the higher value when in contrast to the control were basalt stone powder B2 (50% basalt stone powder + 50% silica sand) geopolymer samples.

Regarding water absorption and porosity effects in contrast to the control sample, the basalt stone mixes improved amelioration in weight loss due to abrasion.

The basalt stone powder is used as a filler material with silica sand in different ratios to produce composites with proper inside traits and applicable interfacial for the geopolymeric matrix.

As an established conclusion, growing waste materials, as a filler replacing silica sand with different ratios, basalt powder concerning the control samples contributed to the mechanical behaviors development of the composite. On the other hand, the use of fly ash and zeolite as a binder material with a ratio of 70% - 30% was given the best result according to other ratios used in the trail mixes.

References

[1] Célerier, S., Morisset, S., Batonneau-Gener, I., Belin, T., Younes, K., & Batiot-Dupeyrat, C. (2018). Glycerol dehydration to hydroxyacetone in gas phase over copper supported on magnesium oxide (hydroxide) fluoride catalysts. Applied Catalysis A: General, 557, 135-144. https://doi.org/https://doi.org/10.1016/j.apcata.2018.03.022

[2] Chakkor, O., & Altan, M. F. Metakaolin and Red-Mud Based Geopolymer: Resistance to Sodium and Magnesium Sulfate Attack. Celal Bayar University Journal of Science, 17(1), 101-113.

[3] Chen, L., Willis, S. N., Wei, A., Smith, B. J., Fletcher, J. I., Hinds, M. G., Colman, P. M., Day, C. L., Adams, J. M., & Huang, D. C. S. (2005). Differential Targeting of Prosurvival Bcl-2 Proteins by Their BH3-Only Ligands Allows Complementary Apoptotic Function. Molecular Cell, 17(3), 393-403. https://doi.org/https://doi.org/10.1016/j.molcel.2004.12.030

[4] Criado, M., Fernández-Jiménez, A., & Palomo, A. (2010). Alkali activation of fly ash. Part III: Effect of curing conditions on reaction and its graphical description. Fuel, 89(11), 3185-3192. https://doi.org/https://doi.org/10.1016/j.fuel.2010.03.051

[5] Cyr, M., & Pouhet, R. (2015). 15 - Resistance to alkali-aggregate reaction (AAR) of alkali-activated cement-based binders. In F. Pacheco-Torgal, J. A. Labrincha, C. Leonelli, A. Palomo, & P. Chindaprasirt (Eds.), Handbook of Alkali-Activated Cements, Mortars and Concretes (pp. 397-422). Woodhead Publishing. https://doi.org/https://doi.org/10.1533/9781782422884.3.397

[6] Davidovits, P., Jayne, J. T., Duan, S. X., Worsnop, D. R., Zahniser, M. S., & Kolb, C. E. (1991). Uptake of gas molecules by liquids: a model. The Journal of Physical Chemistry, 95(16), 6337-6340. https://doi.org/10.1021/j100169a048

[7] Dupuy, T. J., Brandt, T. D., Kratter, K. M., & Bowler, B. P. (2019). A Model-independent Mass and Moderate Eccentricity for β Pic b. The Astrophysical Journal, 871(1), L4. https://doi.org/10.3847/2041-8213/aafb31

[8] Duxson, P., Provis, J. L., Lukey, G. C., & van Deventer, J. S. J. (2007). The role of inorganic polymer technology in the development of 'green concrete'. Cement and Concrete Research, 37(12), 1590-1597. https://doi.org/https://doi.org/10.1016/j.cemconres.2007.08.018

[9] Elder, R. W., Quaegebeur, J. M., Bacha, E. A., Chen, J. M., Bourlon, F., & Williams, I. A. (2013). Outcomes of the infant Ross procedure for congenital aortic stenosis followed into adolescence. The Journal of Thoracic and Cardiovascular Surgery, 145(6), 1504-1511. https://doi.org/https://doi.org/10.1016/j.jtcvs.2012.09.004

[10] Fu, D., Calvo, J. A., & Samson, L. D. (2012). Balancing repair and tolerance of DNA damage caused by alkylating agents. Nature Reviews Cancer, 12(2), 104-120. https://doi.org/10.1038/nrc3185

[11] Gharzouni, A., Ouamara, L., Sobrados, I., & Rossignol, S. (2018). Alkali-activated materials from different aluminosilicate sources: Effect of aluminum and calcium availability. Journal of Non-Crystalline Solids, 484, 14-25. https://doi.org/https://doi.org/10.1016/j.jnoncrysol.2018.01.014

[12] Hajjaji, W., Andrejkovičová, S., Zanelli, C., Alshaaer, M., Dondi, M., Labrincha, J. A., & Rocha, F. (2013). Composition and technological properties of geopolymers based on metakaolin and red mud. Materials & Design (1980-2015), 52, 648-654. https://doi.org/https://doi.org/10.1016/j.matdes.2013.05.058

[13] He, J., Jie, Y., Zhang, J., Yu, Y., & Zhang, G. (2013). Synthesis and characterization of red mud and rice husk ash-based geopolymer composites. Cement and Concrete Composites, 37, 108-118. https://doi.org/https://doi.org/10.1016/j.cemconcomp.2012.11.010

[14] He, J., Zhang, J., Yu, Y., & Zhang, G. (2012). The strength and microstructure of two geopolymers derived from metakaolin and red mud-fly ash admixture: A comparative study. Construction and Building Materials, 30, 80-91. https://doi.org/https://doi.org/10.1016/j.conbuildmat.2011.12.011

[15] Kamseu, E., Nait-Ali, B., Bignozzi, M. C., Leonelli, C., Rossignol, S., & Smith, D. S. (2012). Bulk composition and microstructure dependence of effective thermal conductivity of porous inorganic polymer cements. Journal of the European Ceramic Society, 32(8), 1593-1603. https://doi.org/https://doi.org/10.1016/j.jeurceramsoc.2011.12.030

[16] Kenne Diffo, B. B., Elimbi, A., Cyr, M., Dika Manga, J., & Tchakoute Kouamo, H. (2015). Effect of the rate of calcination of kaolin on the properties of metakaolin-based geopolymers. Journal of Asian Ceramic Societies, 3(1), 130-138. https://doi.org/https://doi.org/10.1016/j.jascer.2014.12.003

[17] Kong, D. L. Y., Sanjayan, J. G., & Sagoe-Crentsil, K. (2007). Comparative performance of geopolymers made with metakaolin and fly ash after exposure to elevated temperatures. Cement and Concrete Research, 37(12), 1583-1589. https://doi.org/https://doi.org/10.1016/j.cemconres.2007.08.021

[18] Krivenko, A. G., Komarova, N. S., & Piven', N. P. (2007). Electrochemical generation of solvated electrons from nanostructured carbon. Electrochemistry Communications, 9(9), 2364-2369. https://doi.org/https://doi.org/10.1016/j.elecom.2007.07.004

[19] Nikolić, V., Komljenović, M., Baščarević, Z., Marjanović, N., Miladinović, Z., & Petrović, R. (2015). The influence of fly ash characteristics and reaction conditions on strength and structure

of geopolymers. Construction and Building Materials, 94, 361-370. https://doi.org/https://doi.org/10.1016/j.conbuildmat.2015.07.014

[20] Oh, J. E., Monteiro, P. J. M., Jun, S. S., Choi, S., & Clark, S. M. (2010). The evolution of strength and crystalline phases for alkali-activated ground blast furnace slag and fly ash-based geopolymers. Cement and Concrete Research, 40(2), 189-196. https://doi.org/https://doi.org/10.1016/j.cemconres.2009.10.010

[21] Ranjbar, N., Mehrali, M., Mehrali, M., Alengaram, U. J., & Jumaat, M. Z. (2015). Graphene nanoplatelet-fly ash based geopolymer composites. Cement and Concrete Research, 76, 222-231. https://doi.org/https://doi.org/10.1016/j.cemconres.2015.06.003

[22] Zhang, Z., Provis, J. L., Reid, A., & Wang, H. (2014). Geopolymer foam concrete: An emerging material for sustainable construction. Construction and Building Materials, 56, 113-127. https://doi.org/https://doi.org/10.1016/j.conbuildmat.2014.01.081

INTERNATIONAL JOURNAL OF ELECTRONICS, MECHANICAL AND MECHATRONICS ENGINEERING
Vol.10 Num.2 - 2020 (1785 - 1789)

Renewable Energy as Solution to Energy Deficiency in Burundi

Samuel MACUMI[1] , Mehmet Emin TACER[2]

Abstract

This study focused on the electrification of Burundi and how to equip Burundi with enough energy. Burundi is a member of various economic communities such as the East African Community (EAC), the Common Market for the East and South Africa (COMESA,) and the Economic Community of the Great Lake Countries (CEPGL). Burundi is still one of the poorest countries in the world, although it is a member of many economic communities. The most sensitive cause of this poverty situation is the lack of energy which slows down almost the entire economic chain.

In this study, using the natural (renewable) energy sources of Burundi, the development of the source of electric energy that influences the development of the country has been taken into consideration. As a result of this research, due to the geographical position of Burundi, solar energy was on focus as the most suitable energy source among renewable energy sources. In this context, it is envisaged to provide the transportation of electric energy to all regions that are not still used in electricity, and thus increase both economy and lifestyles.

Following this study, the Burundi Government, the Burundi economy operators, various partners, and investors will be able to overcome the development challenges and, as a result, this will lead to the improvement of this energy field, which is considered the pillar of a sustainable socioeconomic element in a worldwide area.

Keywords: *Solar energy, landlocked country, energy power, power plant, renewable energy, energy supply, energy deficiency.*

[1]*Electrical Electronics Engineering, Engineering Faculty, Istanbul Aydin University, Istanbul, Turke y, e-mail sammacumi@gmail.com*
[2]*Electrical Electronics Engineering, Engineering Faculty, Istanbul Aydin University , Istanbul, Turkey, e-emintacer@aydin.edu.tr*
DOI: 10.17932/IAU.IJEMME.2010.001/ijemme_v10i2003

1. Introduction

Burundi is located in Eastern Africa and extends between 28°58 'and 30°53' east longitude and between 2°15 'and 4°30' south latitude. It is bounded by Rwanda in the North, the Democratic Republic of Congo (DRC) in the West, and Tanzania in the South and East. It covers an area of 27834 km^2 of which about 2000 km^2 are occupied by the Burundian part of Lake Tanganyika and the population is 11,099,298 [1].

The majority of the Burundian population lives in the countryside and access the electric energy remains very low. The rural population is estimated about 90 percent [2]. Less than 5% of the population has access to the national grid. This implies a huge consumption of fuel wood as a source of primary energy, thus presenting serious negative consequences for the environment. Traditional biomass alone presents 99% of which 70% comes from firewood, 18% comes from agricultural residuals, 6% comes from coal, and 1% comes from bagasse [3].

The Burundian population living in the countryside needs to obtain basic energy; an essential energy especially for cooking and other activities requiring heating. This energy is obtained mainly from the combustion of biomass including firewood and charcoal. Despite this variety in energy sources, firewood and coal come first with a share of around 97.5% of Burundi's overall energy consumption, while the remaining 2.5% is between electricity and oil [1]. The Burundian population lives mainly in the countryside and therefore has no access to the national electricity Grid. It is a population with a growth rate varying between 0% and 4% if we take into account the forecast of the population evolution from 2005 to 2045 [2].

Table 1: Prediction of Burundian population horizon 2045[2]

Year	Population	Density (Km^2)	Growth Rate
2005	7,423,289	266.70	3.01%
2010	8,766,930	314.97	3.38%
2015	10,199,270	366.43	3.07%
2020	11,939,227	428.94	0.00%
2025	13,810,006	496.16	2.95%
2030	15,798,849	567.61	2.73%
2035	17,970,195	645.62	2.61%

With the increase in the population, the energy consumption has increased so much that the energy system of Burundi has become weak due to the enormous energy demand. Also, the energy demands caused by rapid urbanization and the creation of industries and activities requiring electrical energy have led to the insufficiency of the Burundi 's energy system.

The amount of electricity being consumed in Burundi comes from the production of hydroelectric power stations and thermal plant built in Burundi. There are other news hydro power plants being built like Jiji Murembwe and Mpanda hydroelectric plant while another part of the electricity is imported from neighbouring countries power plants such as RUZIZI 1 and RUZIZI 2 in the Democratic Republic of Congo. Another important quantity of electricity will be imported from the RUSUMO FALLS hydroelectric power plant, which is being built between Burundi, Rwanda and Tanzania.

Despite this energy deficiency, Burundi's hydroelectric potential is 1700MW, of which 300MW are economically exploitable, but only 32 MW are developed [7,13]. Solar potential is estimated at an annual average of sunshine of 2000 KWh/.year; equivalent to the sunniest European regions of the Mediterranean [7,13]. However, despite all these potential energy supplies, Burundi has such a severe energy crisis that has a major impact on its ability to reduce poverty and achieve the Millennium Development Goals (MDGS).

Considering the current energy situation in Burundi; the little energy available in Burundi comes mainly from hydroelectric plants, fuel, solar energy, biomass, peat, firewood, coal, bagasse and wind energy.

Thermal Energy: In Burundi, thermal plants are less frequent. These use hydrocarbons as fuel. They are so expensive when compared with hydroelectric plants.

Solar Energy: By its geographical position, Burundi is one of the sunny countries throughout the year. The study conducted in 2013 by the Ministry of Energy and Mines of Burundi with the support of the United Nations Development Program in Burundi (UNDP) on the Diagnostic of the Energy Sector in Burundi in the framework of the initiative of the United Nations Secretary-General on Sustainable Energy for. However, despite this excellent solar distribution, this energy form is not exploited to the maximum. Some individuals, some hospitals and health centre, some schools, some rural households exploit this energy form using photovoltaic panels.

The Peat: The National Peat Office (ONATOUR) in the country has the mission to exploit and commercialize production and use of peat; primarily in industry and agriculture and conduct further research and studies of the peat potential

Bagasse: Bagasse is an efficient source of energy but not enough in Burundi. Only SOSUMO (Société Sucrière de Moso) has an electric power plant powered by biomass from bagasse. This power station of SOSUMO is a form of cogeneration unit fed by the residues of sugar cane known as bagasse.

Biogas: As defined by the book entitled "LIVRE BLANC DU BIOGAZ", biogas is an energy derived from the degradation of organic matter.

Firewood: In Burundi, wood in its raw form or in the form of coal is the main source of energy for cooking and other craft and commercial activities requiring heating.

2. Renewable Energy Resources: Solar Energy

All electrical power installed in Burundi remains below 100 MW. Demand is far higher than supply. The minimum power required by 2020 is of the order of 280 MW, whereas the new programs in progress expect to reach only about 180 MW more by this time; energy requirements for the mining sector are estimated between 300 and 800 MW in the next 10 years for the nickel industry alone and its associated minerals; the electrical installations are very old and cause a lot of losses [1]. The solar field of Burundi is very interesting. The average sunshine received annually is close to 2,000 kWh / m^2 year which is equivalent to the best European regions (southern Mediterranean) [20]. Despite the significant cloudiness due to the equatorial situation of Burundi and periods of rain, the exploitation of solar energy in Burundi is therefore an interesting solution to electrical energy deficiency. The

production of electricity by solar energy can be achieved by photovoltaic technology or by thermal solutions. In the case of Burundi, only the photovoltaic option seems appropriate [20].

The different visions of the Republic of Burundi, whether Vision 2025, Vision 2045, and others, predict that Burundi will no longer be among the poorest countries but rather among the emerging countries. In this way, the energy sector is one of the key sectors for this change.

2.1 Implementation of The Solar Photovoltaic System in Burundi's Energy System

Taking into account the solar photovoltaic system in Burundi's vision for energy between 2020 and 2045 years, as a response to the Millennium of Development Goals, the largest number of people is planning to work in the electricity sector. An estimated inventory for the electrical load of all categories of consumers registered in Burundi's electricity grid as added to the existing one is made to be able to build the photovoltaic power plants that could considerably reduce the electricity shortage that Burundi faces. Thus, for households, villages, and neighborhoods, the electricity consumption forecasts for the next 10 years, 20 years, 30 years, etc. seemed to be resolved.Taking into account the data in the table of the projection of the population growth, it is enough to make an estimated inventory of the needs in electrical energy for a household considered modern and after to multiplying by the estimated number of households which can constitute a village or a modern neighborhood. However, as the population continues to increase, it will be sufficient to increase energy production according to new villages and neighborhoods that will be created as electricity consumption of a village, the modern neighborhood will be known (Table 2).

For the other categories of consumers, the forecast of electricity consumption also seems not to be complicated. The tables of the evolution of the electric consumption and the evolution of the number of subscribers for the 10 years run, give an idea of what will look like the consumption of electricity in the years to come (Table 3).

Table 2: Estimated Daily Electrical Load Table for a Single Modern Household and a Modern Village [1]

Watts-hour/per	Equipment	No. in use	Power(w)	Total Power	Hours/Day	Watt-hour/day
1	Lamps LED	12	5	60	6	360
2	Cell-Phones	3	5	15	3	45
3	Radios	1	10	10	8	80
4	Televisions	1	40	40	6	240
5	Refrigerators	1	75	75	20	1500
6	Iron	1	1000	1000	0.25	250
7	DVD Player	1	30	30	2	60
8	Water pumps	1	500	500	1	500
9	computer	1	100	100	3	300
10	Washing machine	1	2000	2000	0.25	500
Total						3835
No. of Households						100
Total for households						383500

During this study, a projection of the evolution of the Burundian population as well as its estimated energy consumption horizon 2045 following the Millennium Development Goals were made in order to allow any project developer to take this into account. The sun being available and emitting radiation everywhere in Burundi, it could contribute enormously in the increase of the electric energy in Burundi as it was found in this study. The solar potential of Burundi can be estimated at 5 kWh / m² / day in the Bujumbura region and 4 kWh / m² / day for the highlands. This potential offers the opportunity to build solar power plants connectable to the grid and can be photovoltaic type or thermal type.

To meet at least the needs of different subscribers in electricity and to give access to electricity to as many Burundians as possible, an installed electrical power estimated at **345.7 GWh** could be implemented by 2023 while the estimated power of **617.9 GWh** could be installed for 2032. Going beyond, a nearby installed electrical power of **1234.2 GWh** could be implemented by 2045.

It has been determined, so that households have the living standards that meet the Millennium Development Goals, a daily energy consumption of a modern neighbourhood should be 383500 watts-hour/day. The following example of a photovoltaic power station can be used to provide electricity in about 8 neighbourhoods with 100 modern households each one.

The storage capacity needed depends essentially on 2 parameters: the energy consumed per day and the autonomy of the system, that is to say the number of days that it will be able to support without sun.

Table 3: Recapitulative table of estimated daily electricity consumption for all categories of subscribers of the Burundi energy system horizon 2023, 2032, 2041 (in GWh)

Consumer categories	2005	2014	2023	2032	2041
Government	4.3	6.1	7.9	11.5	18.7
Common and public lighting	0.5	1.3	2.1	3.7	6.9
Trade	12.0	33.7	55.4	98.8	185.6
Industries and Craft	1.6	33.3	65.0	128.4	255.2
Households	45.9	105.3	164.7	283.5	521.1
REGIDESO	1.0	4.9	8.8	16.6	32.2
International Organizations	2.5	1.2	1.0	2.0	1.5
State Corporations	1.0	10.6	20.2	39.4	77.8
Administration, personalized management	3.4	12.5	21.5	39.6	75.8
Religious confessions and social organizations	2.9	4.3	5.7	8.5	14.1
Prepaid sales	4.7	9.8	14.9	25.1	45.5
Total	79.8	223	345.7	617.9	1234.2

Determination of desired autonomy

Autonomy generally varies between 3 and 15 days. Therefore, a higher autonomy is chosen to ensure the continuity of the activity: between 5 and 7 days, therefore a weak autonomy for 5 days is estimated and then the amount of energy consumed by the facility during the given time is as follows:

$$Eft = Dn \bullet Au = 3\ \text{MWh x 5 days } \_15\ MW\text{h}. \quad (1)$$

The amount of energy that will have to be returned by the batteries is therefore, choosing inverter efficiency is 0.9):

$$ERb = Ec = \text{- (1-losses in line)} = 3/(0.9\text{x}0.97 = 3.436\ \text{MWh} \quad (2)$$

For our installation is taken as the maximum depth of discharge of 50%, the capacity of the batteries must therefore be:

$$C_B = Er/Maxxdd = 3.436\text{MWh}/0.5 = 6.872\text{MWh} \quad (3)$$

Batteries with voltage of 24V and capacity of 200Ah:

6.872MWh x 1000000 = 6872000 Wh

6872000/24 = 286333.333Ah

286333.333/200Ah = 1431.6665

Therefore; 1432 batteries of 24V is required.

Calculating total Watt-hours per day needed from the PV modules.

After carefully calculating the electrical energy consumed by each device connected to the system, calculating the total number of watt hours requested from the photovoltaic modules becomes simple.

Total watt hour from the photovoltaic modules;

$$E\_Pm = \Sigma\ E\ *1.3Lt \equiv \Sigma\ (P*t)*1.3Lt \quad (4)$$

where ∑E is the sum of the amount of energy consumed by each device in the system
Lt is the total losses that could happen in the system installations, t is working time per day.

Sizing of the PV modules:

Photovoltaic modules produce different amounts of power depending on whether their size and the material from which they are manufactured differ. Indeed, before pretending to know the sizing of the photovoltaic module, the determination of the total requirements in watt peak to be produced is an obligation.

Calculating of the total Watt-peak rating needed for PV modules:

During this step, the total peak power required for the PV panels must be determined to ensure the operation of the devices.

(5)

Where P_{Rp} is the Rated Peak Power, P_{Wpd} is the daily peak power (watts-peak/day) and PV_{Gfp} the generation factor of the photovoltaic panels

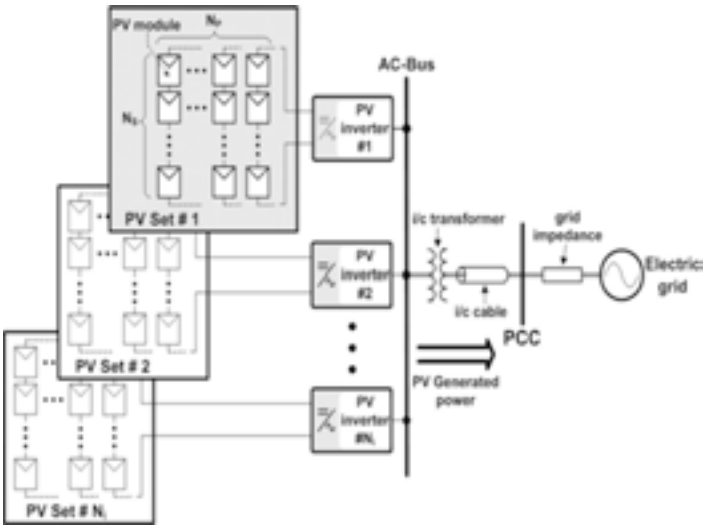

Fig.1 Block diagram of the large PV plant [31].

Calculating of the number of PV panels for the system:

A block diagram of the large PV plant that is considered in the proposed optimization process is illustrated in Fig. 1.

The PV modules are distributed in multiple PV inverters, and the generated power is injected into the electric grid at the point of common coupling (PCC) through an interconnection (i/c) transformer and cable, respectively. The total number of PV modules which must be installed in the PV plant $N_{1,o}$ is calculated according to the PV plant power rating $P_{plant,\ nom}$ (MW p) that is specified by the PV plant designer, as follows:

$$N_{I,O} = \frac{P_{Plant,nom}}{P_{M,STC}} .10^6 \qquad (6)$$

where $P_{m,stc}$ (W) is the power rating of each PV modüle.

3.CONCLUSION

During this study, a projection of the evolution of the Burundian population, as well as its estimated energy consumption horizon of 2045 following the Millennium Development Goals were made in order to allow any project developer to take this into account. The sun being available and emitting radiation everywhere in Burundi, could contribute enormously to the increase of the electric energy in Burundi as was found in this study. The solar potential of Burundi can be estimated at 5 kWh / m2 / day in the Bujumbura region and 4 kWh / m2 / day for the highlands. This potential offers the opportunity to build solar power plants connectable to the grid and can be the photovoltaic type or thermal type.

REFERENCES

[1] Aras H et al (2004) Multi-criteria selection for a wind observation station location using analytic hierarchy process. Renew Energy 29:1383–1392.

[2] Lee SK et al (2009) Decision support for prioritizing energy technologies against high oil prices: a fuzzy analytic hierarchy process approach. J Loss Prev Process Ind 22:915–920

[3]Afgan NH, Carvalho MG (2002) Multi-criteria assessment of new and renewable energy power plants. Energy 27:739–755

[4]Cavallaro F (2009) Multi-criteria decision aid to assess concentrated Samouilidis J, Mitropoulos C. Energy economy models—a survey. European Journal of Operations Research 1982;25:200–15.

[5]Meirer P, Mubayi V. Modeling energy-economic interactions in developing countries-a linear programming approach. European Journal of Operations Research 1983;13:41–59.

[6]Nijcamp P, Vwolahsen A. New directions in integrated energy planning. Energy Policy 1990;18(8):764–73.

[7]Kavrakoglu I. Multi-objective strategies in power system planning. European Journal of Operations Research 1983;12:159–70.

[8]Schulz V, Stehfest H. Regional energy supply optimization with multiple objectives. European Journal of Operations Research 1984;17:302–12.

[9]Putrus P. Accounting for intangibles in integrated manufacturing-non-financial justification based on analytical hierarchy process. Information Strategy 1990;6:25–30.

[10]Boucher TO, McStravic EL. Multi-attribute evaluation within a present value framework and its relation to analytic hierarchy process. The Engineering Economist 1991;37:55–71.

[11]Ozelkan EC, Duckstein L. Analyzing water resources alternatives and handling criteria by multicriterion decision techniques. Journal of Environmental Management 1996;48:69–96.

INTERNATIONAL JOURNAL OF ELECTRONICS, MECHANICAL AND MECHATRONICS ENGINEERING
Vol.10 Num.2 - 2020 (1791 - 1800)

Investigation of Improvement Methods in Existing Defective Building Stocks

Mehmet Fatih ALTAN[1], Alaa Abed Al Kareem Safhan ALRWASHDEH[2]

Abstract

The use of nonlinear analysis methods in strengthening structures has become increasingly important in recent years. In the first part of this thesis, major strengthening methods are outlined without going into detail. Furthermore, a model building with fire damage was modeled with ETABS and a method was proposed. In addition, the building was analyzed in detail using the finite element model using SAP2000. Shear walls used for reinforcement with modal analysis and push analysis were designed. Approaches are needed to increase structural safety of structural members after fire. Fiber reinforced polymer (FRP) is increasinglyused in civil engineering applications regarding its excellent strength/weight ratio and anti-corrosion ability. Existing experimental research on the performance of fire-damaged RC elements repaired with concrete coating, steel coating and fiber-reinforced polymer (FRP) coating has been reviewed.

Keywords: *Pushover Analysis, Modal Analysis, Shear Wall, Reinforcement, Seismic Performance.*

1. Introduction

Construction in Afghanistan is very different from construction in the US and offers many challenges to maintain good quality. The availability (or lack) of materials and equipment determines most construction methods. Outside major cities, building designs rarely had any impact on earthquake forces historically, but old methods were followed without any modern building code effect. There are no special building codes for Afghanistan, foreign laws and standards are used for the construction of buildings, roads, highways and bridges. This prevented the private sector from investing in buildings in Afghanistan without any official code. This policy will lay the groundwork for the future development of rules, regulations and building codes in the city of Kabul.

[1]*Prof., Department of Civil Engineering, Istanbul Aydin University, Istanbul, Turkey, e-mail: mehmetaltan@aydin.edu.tr*
[2]*Department of Civil Engineering, Istanbul Aydin University, Istanbul, Turkey.*
DOI: 10.17932/IAU.IJEMME.2010.001/ijemme_v10i2004

1.1. General Finite Element Analysis of The Building

In the last decade, the computer application for structural analysis has been greatly developed. The Finite element method has been proved to be very accurate for static and dynamic analysis for the different types of structural modeling. Two Finite element and matrix models have been used for the Building analysis. In these models the structural components of Building are considered as three-dimensional frame element. The Building system is idealized and modeled using three-dimensional frame element with 6 degrees of freedom for each node for quick check of main displacement and stress control. The geometric characteristics of the Building and its various elementsare modeled and determined on the basis of the planned geometric layout. The geometrical and inertial properties foreach member of the Building system are computed as a whole and analysis were done. In this study SAP2000 and ETABS is used as finite element program and matrix. The elements that used in modeling the Building are three-dimensional Frame Elements which represents column and beam elements together with shell element that representthe floor slab and shear walls. Detailed descriptions of these elements are discussed in the following sections. Three-dimensional frame element is a two-node prismatic linear element based on three-dimensional beam-column formulations. It has a twelve-degree of freedoms and it is capable of resisting axial forces, shear forces and bending moments about the two principal axes in the plane of its cross section, and twisting moments about its longitudinal axis. The material properties of the beam-column element are the elastic modulus E, and shear modulus G. The geometrical properties of the element are defined locally and included cross sectional area A_X, shear Areas A_y, A_Z, moments of inertia I_{yy}, I_{ZZ} and torsional moment of inertia J_r. The local coordinate system used for frame element is presented in Figures.

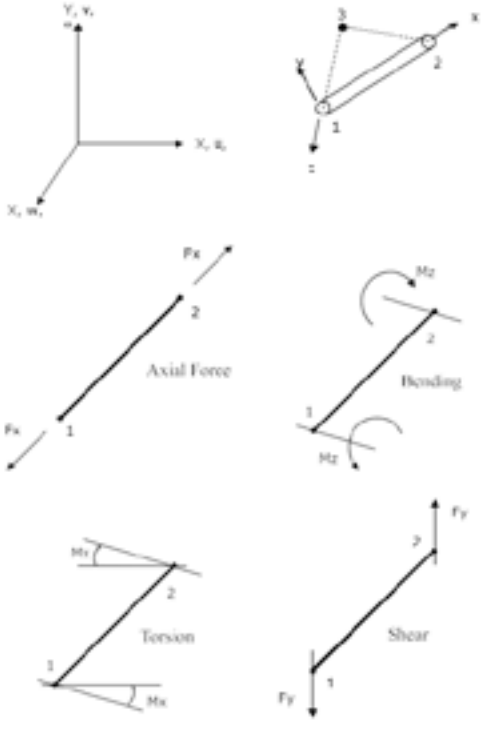

Figure 1: Three dimensional frame element with 6 degrees of freedom

Table 1: The element local forces in the local coordinates.

NAME	*EXPLANATION*	*UNIT*
Fx :	Axial Force (kN)	(kN)
Fy :	Shear Force in y-direction (kN)	(kN)
Fz :	Shear Force in z-direction (kN)	(kN)
Mx :	Torsion (kN.m)	(kN.m)
My :	Moment in xy-plane (kN.m)	(kN.m)
Mz :	Moment in yz- plane (kN.m)	(kN.m)

Sign convention for the frame element used in the analysis can be summarized as:

Table 2: Sign convention of beam element

Sign convention of beam element		
Axial Force	(positive)	Axial Tension
	(negative	Axial compression
Bending moment	(positive)	Hogging moment
	(negative)	Sagging moment
Torsion	(positive)	Anti-clockwise rotation (1st node), clockwiserotation (3rd node)
	(negative)	Clockwise rotation (1st node), anti-clockwiserotation (3rd node)

In the full Building model all elements are modeled as frame elements. All Building elements are made of concrete which its related properties are given in the following tables.

Table 3: Elastic Material Properties

Building Part	**Elasticity Modulus, E, kN/m²**	**Unit Weight, ρ (Ton/m3**	**Poisson Ratio, ν**
All Rebars	$210*10^6$	8.0	0.3
Concrete 116	$25*10^6$	2.4	0.2
Concere 250	$25*10^6$	2.4	0.2

To achieve more accurate results, the structural components of the Building have been modeled as beam elements. This model is used for the static, dynamic, natural frequency analysis. The geometric characteristics of the Building and its various elements are modeled and determined on the basis of the planned geometric layout. The support ends of the Building are assumed to

be simple supported. They are generally located as contact face of wheels. The finite element discretization includes 2000 nodes, 3000 frame and 3000 shell elements.

1.2. Definitions of The Applied Loads on The Building System

The Building system is exposed to different type of applied external and internal loads. The loads acting on the Building in its operating and non-operating conditions include the loads due to the dead weight, the wind load, and the dynamic loads caused by earthquake. At the end of this section the general views of each load cases are given.

The dead load is calculated by program automatically by using the cross sectional properties as area multiplied by length and the density of concrete and adde load as the 170 Kg/m^2. The live load is computed by assuming total loadsof slabs and the Live load is also as taken of 500 kg/m^2. Buildings and other structures, including the Main Wind-

Force Resisting System (MWFRS) and all components and cladding thereof, shall be designed and constructed to resist wind loads as specified herein. The wind load to be used in the design of the MWFRS for an enclosed or partiallyenclosed building or other structure shall not be less than 10 lb/ ft2 (0.48 kN/m^2) multiplied by the area of the buildingor structure projected onto a vertical plane normal to the assumed wind direction [1]. The design wind force for open buildings and other structures shall be not less than 10 lb/ft^2 (0.48 kN/m^2) multiplied by the area Af.

$$p = q(GC_f q_j(GC_{pi}) \text{ (lb/ft}^2\text{) (N/m}^2\text{)} \quad (1)$$

Design and wind pressures for all buildings with h > 60 ft (18.3 m) will be determined from the equation above. According to the seismic map of a report from USGS and USAID, “preliminary earthquake hazard map of Afghanistan”, Kabul has a 2% chance in 50 years of exceeding a peak ground acceleration of 50% gravity respectively, and a 10% chance in 50 years of exceeding a peak ground acceleration of 27% gravity respectively. The designers considered 0.3g for base ground acceleration because this construction is not included in special constructions for %2chance in 50 years. Response spectrum analysis seeks to estimate the maximum response of the structure under earthquake excitation without recourse to direct integration of the model over the complete duration of the earthquakeand scaled to 1g. Response spectrum analysis assumes that the structure behaves linearly. The aim of the investigation conducted herein is to find out the initiation of maximum stress zones in the Building.

(a)

Mode	Period (sec)	Ux	Uy
1	1.93	0.0033	39.8455
2	1.77	39.3769	0.0088

Maximum Diaphragm CM Displacement & Rotation	Value
Ux (cm)	69.9
Uy (cm)	79.8
Rz (Radian)	0.012

Drift	Value
X direction	0.03
Y direction	0.04

(b)

Figure 2: (a) Existing structure (b) Existing structure analysis

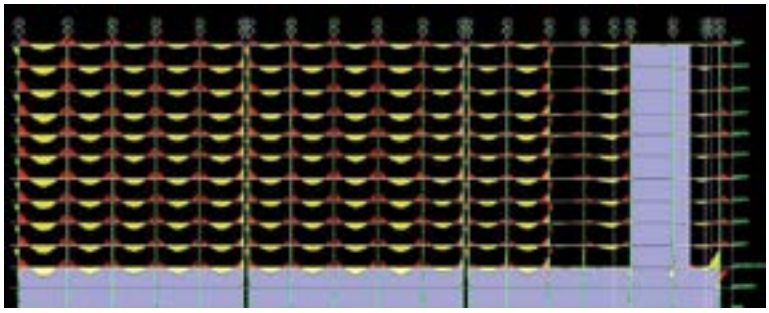

Figure 3: Moment 3-3 diagram

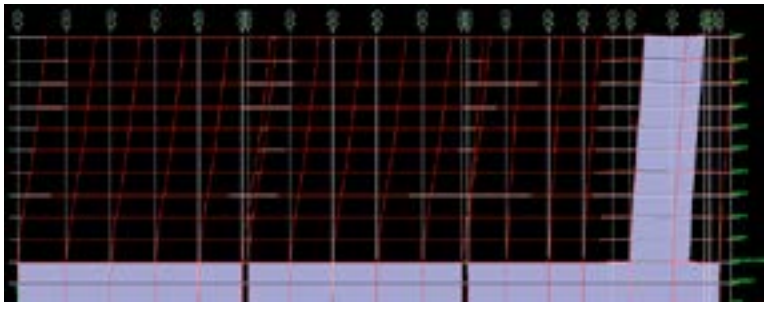

Figure 4: Deformed shape for spectral loading

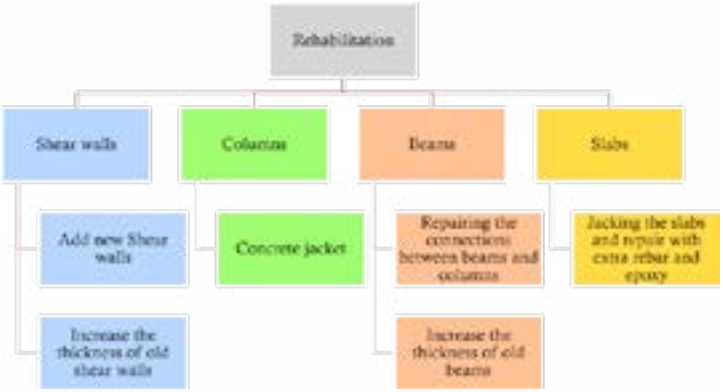

Figure 5: Rehabilitated

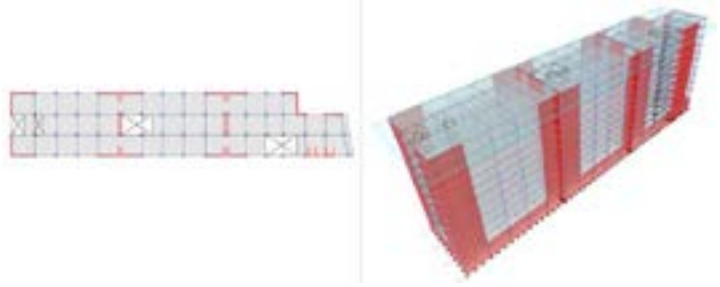

Figure 6: Rehabilitated structure

1.3. Modal Analysis of Building

For detailed consideration, a few mode shapes are shown in 3D and plan views and a little explanation is worth mentioning. Due to to the special design of this Building mode shapes are rather different than the ordinary building.

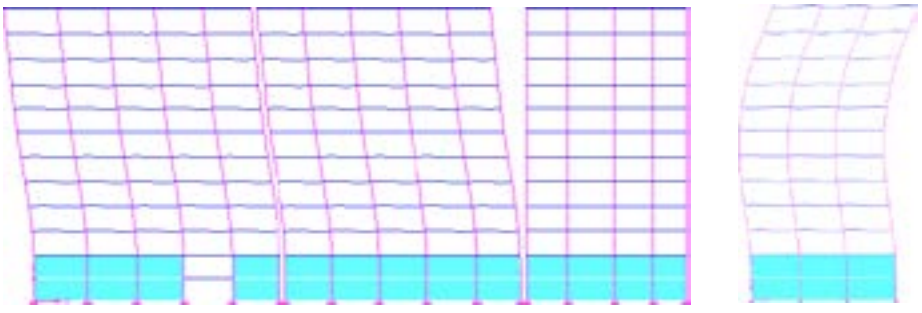

(a) (b)

Figure 7: (a) Mode 2, Period 1.78 sec (b) Mode 7, Period 0.7 sec

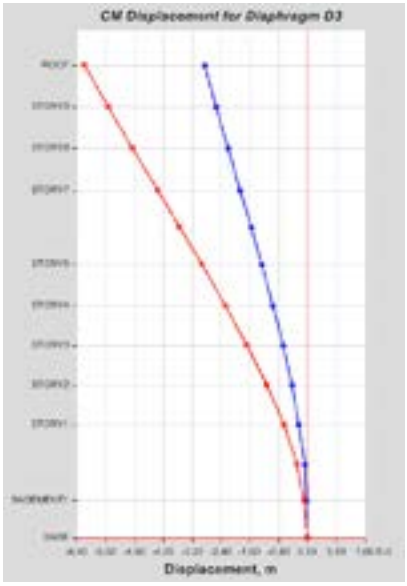

Figure 8: Center of mass displacement for diaphragm D3

1. Materials and Methods

For modeling and analysis of this construction, ETABS software was used. According to test of available construction, specified concrete compressive strength 11.6 Mpa and modulus of elasticity 2551461 has been modeled and all typesof shear walls and columns and beams drawn in the software. For this project we have 3 types of loading as: Dead load, Live load, Earthquake. According to ACI318 all of the load combinations have been known for software. Of course, earthquake loading modeled for X direction and Y direction and for both of them ±5% eccentricity, because this construction may be having torsion side force. Therefore, has been analysis.

Assignment

There are many cracks in the columns and beams, so according to ACI 318 crack must be considered for components in the property modifier moment of inertia around X and Y. It should be noted that the main structural frame is ordinarymoment frame, therefore according to FEMA 360 Ru = 3.

$$C = \frac{ABI}{R_u} = \frac{0.35 \text{ x} \left(N \text{ x } B_1\right) \text{x } 1.2}{3} = \frac{0.35 \text{ x } 1.087 \text{ x } 1.73 \text{ x } 1.2}{3} = 0.2632$$

$$N - \frac{0.7}{4 \quad T_s}\left(T - T_T\right) + 1$$

Soil type is III: $T_0 = 0.15$, $T_s = 0.7$, $S = 1.75$, $S_0 = 1.1$, $T = 0.05 \text{ x } (H)^{0.9} = 1.1122$ Sec

$$B_1 = (S + 1)\left(\frac{T_s}{T}\right)$$

Dead load is 170 Kg/m^2 and Live load is 500 Kg/m^2.

1.1. Pushover Analysis

When analyzing frame objects, material nonlinearity is assigned to discrete hinge locations where plastic rotation occurs according to FEMA-356 or another set of code-based or user-defined criteria [2]. Strength drop, displacementcontrol, and all other nonlinear software features, including link assignment, P-Delta effect, and staged construction,are available during static-pushover analysis. After adding shearwalls to structure and changing old profile to new according to below:

$$\delta_t = C_0 . C_1 . C_2 . C_3 . S_a . \frac{T_e^2}{4\pi^2} . g \qquad (5)$$

δt = 0.2 m, Sample Column: IO = 0.005, LS = 0.015, CP = 0.02, Sample Beam: IO = 0.01, LS = 0.02, CP = 0.025

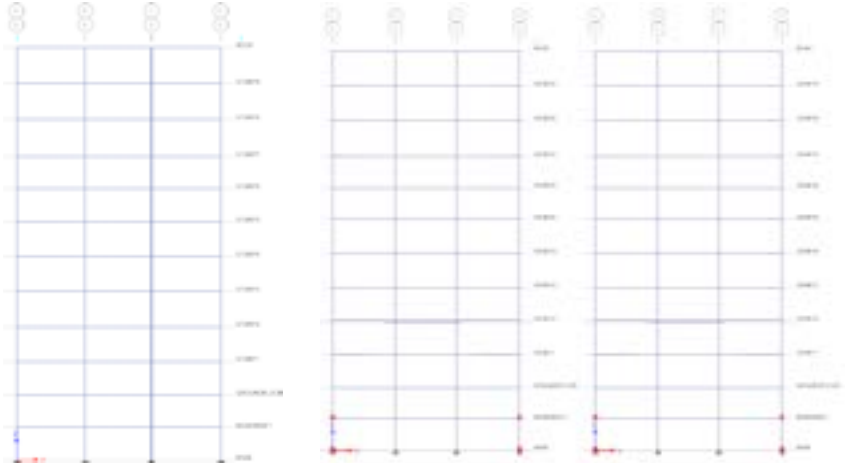

(a) (b) (c)

Figure 9: (a) Step 0 (b) Step 1, Fx=620000 KN (c) Step 2, Fx=910000 KN

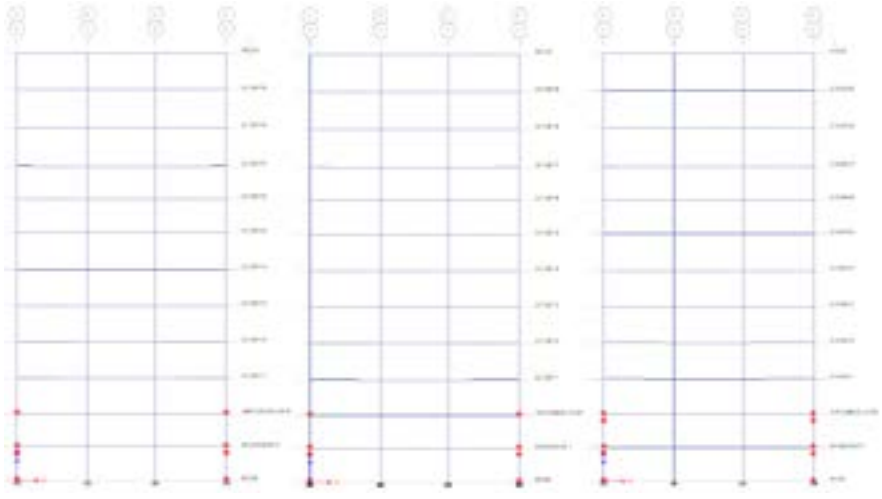

(a) (b (c)

Figure 10: (a) Step 3, Fx=1600000 KN (b) Step 4, Fx=2304000 KN (c) Step 5, Fx=3100000 KN

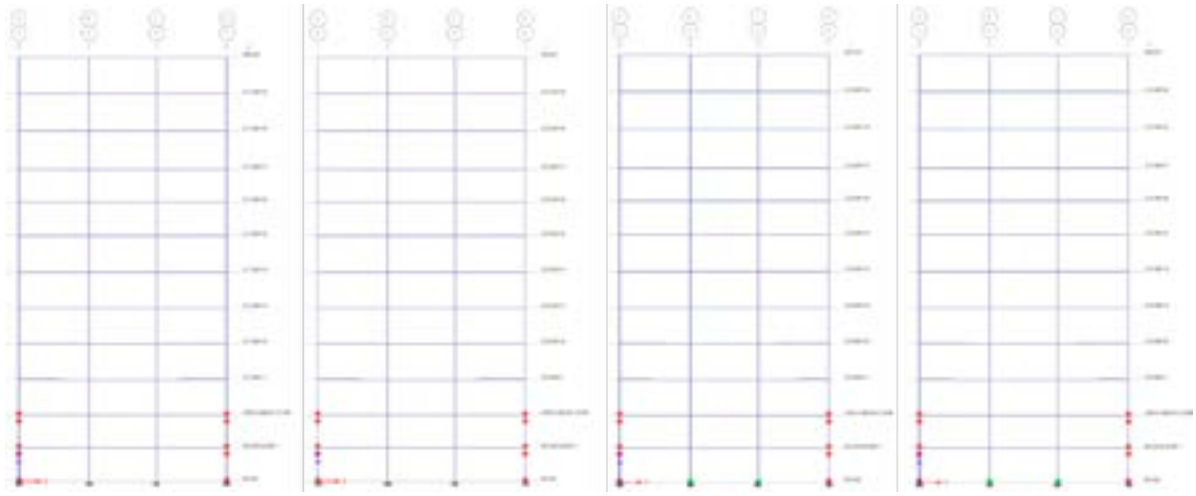

(a) (b) (c)

Figure 11: (a) Step 6, Fx=3962000 KN (b) Step 7, Fx=4888000 KN (c) Step 8, Fx=6000000 KN (d) Step 9,Fx=6206000 KN

2. Conclusion and Suggestions

In the control calculations, the characteristic concrete compressive strength is 8 MPa, and the characteristic yield strength 220 Mpa for longitudinal and transverse reinforcement is taken. Since it is located in the second degree earthquake zone, T_a = 0.15sec, T_b = 0.40 secs were used as ground characteristic periods for A_0 = 0.30 and local ground class Z3. The calculations are based on cracked section stiffnesses. The information level coefficient was taken as 0.90. The building in question was modeled in three dimensions with the existing material quality and ground data and subjected to linear performance analysis.

Comparison: When two plastic joints are created in a column, the column will fail. According to the last slides, the first column in the 3th step will fail, therefore we must compare the equivalent force at this step and maximum base reactionin X direction.

Step 3, Fx=1600000 KN & ELX load combination, ETABS: Fx=172881 KN, IDECAD: Fx=180004 KN

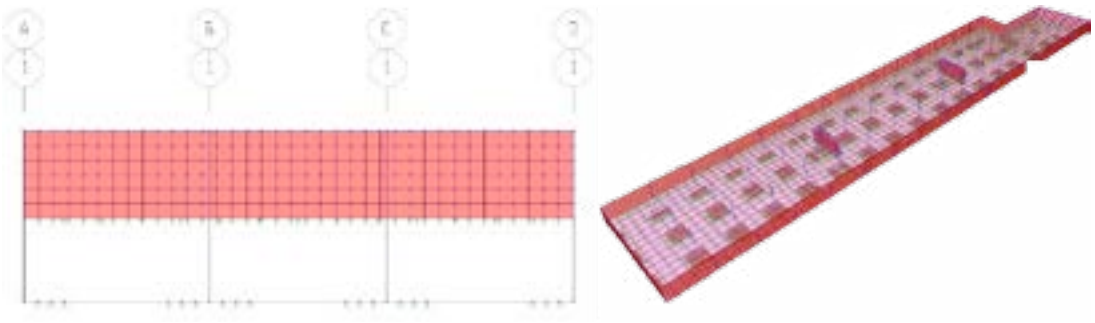

Figure 12: 3D model SAP2000 (Foundation)

As can be seen, some of the columns and beams are below the expected performance, and it is seen that there is a considerable insufficiency in terms of earthquake performance besides the axial force deficiencies in the structure. Various strengthening options have been tried to overcome this situation. According to the preliminary examination calculations, shear wall should be added in both directions in all 3 sections.

Considering the concrete quality, it will be more convenient to coat the columns with FRP. In addition, it should be reinforced with FRP in beams damaged by fire. Compared with steel jacketing and concrete section enlargement, the advantages of FRP jacketing are ease of use, lightness, anti-corrosion and high strength, stiffness / weight ratio. Meanwhile, compared to EBR jacketing, the advantages of FRP jacketing such as better fixation and ductile performance are more obvious [3, 4].

References

[1] American Society of Civil Engineers. (2013). ASCE 7, Minimum Design Loads for Buildings and Other Structures.

[2] FEMA 356 (2000). Prestandard and Commentary for The Seismic Rehabilitation of Buildings.

[3] Fahjan Y., Doran B., Akbas B., Kubin J. (2012). Pushover Analysis For Performance Based-Seismic Design of RcFrames with Shear Walls.

[4] Zhou J., Wang L. (2019). Repair of Fire Damaged Reinforced Concrete Members with Axial Load: A Review.